Materials **2011**, *4*, 601-620; doi:10.3390/ma4040601

OPEN ACCESS

materials

ISSN 1996-1944

www.mdpi.com/journal/materials

Article

Synthesis and Characterization of Self-Assembled Nanogels Made of Pullulan

Sílvia A. Ferreira [1], Paulo J. G. Coutinho [2] and Francisco M. Gama [1,*]

[1] IBB-Institute for Biotechnology and Bioengineering, Centre for Biological Engineering, Minho University, Campus Gualtar 4710-057, Braga, Portugal; E-Mail: silviarmferreira@deb.uminho.pt

[2] Centre of Physics, Minho University, Campus Gualtar 4710-057, Braga, Portugal; E-Mail: pcoutinho@fisica.uminho.pt (P.C.)

* Author to whom correspondence should be addressed; E-Mail: fmgama@deb.uminho.pt; Tel.: (+351) 253 604418; Fax: (+351) 253 678 986.

Received: 4 March 2011 / Accepted: 17 March 2011 / Published: 25 March 2011

Abstract: Self-assembled nanogels made of hydrophobized pullulan were obtained using a versatile, simple, reproducible and low-cost method. In a first reaction pullulan was modified with hydroxyethyl methacrylate or vinyl methacrylate, further modified in the second step with hydrophobic 1-hexadecanethiol, resulting as an amphiphilic material, which self-assembles in water via the hydrophobic interaction among alkyl chains. Structural features, size, shape, surface charge and stability of the nanogels were studied using hydrogen nuclear magnetic resonance, fluorescence spectroscopy, cryo-field emission scanning electron microscopy and dynamic light scattering. Above the critical aggregation concentration spherical polydisperse macromolecular micelles revealed long-term colloidal stability in aqueous medium, with a nearly neutral negative surface charge and mean hydrodynamic diameter in the range 100–400 nm, depending on the polymer degree of substitution. Good size stability was observed when nanogels were exposed to potential destabilizing pH conditions. While the size stability of the nanogel made of pullulan with vinyl methacrylate and more hydrophobic chains grafted was affected by the ionic strength and urea, nanogel made of pullulan with hydroxyethyl methacrylate and fewer hydrophobic chains grafted remained stable.

Keywords: pullulan; synthetic nanogels; self-assembly; amphiphilic macromolecular micelles; Michael addition; hydrophobic domains

1. Introduction

Pullulan is a water soluble, linear, neutral extracellular biodegradable homopolysaccharide of glucose produced by the fungus *Aureobasidium pullulans* (*Pullularia pullulans*) [1-4]. Pullulan consists of maltotriosyl units connected by α-D-1,6-glycoside linkages [3,5]. Pullulan is extensively used in food, cosmetic and pharmaceutical industries because it is easily modifiable chemically, non-toxic, non-immunogenic, non-mutagenic, and non-carcinogenic [5,6]. Furthermore, pullulan has good mechanical properties and attractive functional properties, such as adhesiveness, film formability, and enzymatically-mediated degradability [7]. In the form of self-assembled nanogels, it has been shown to exhibit chaperon like activity, thus being a promising technique for protein refolding [8]. It has been studied as a blood-plasma expander and substitute [9]. Pullulan arose as a promising polymer for various biomedical applications [10], such as surface modification of polymeric materials to improve blood compatibility (bioinert surfaces) [11,12], for gene [13,14] and drug delivery [5,15-19], as a carrier for quantum dots for intracellular labeling to be used as a fluorescent probe for diagnostic bioimaging [20] and tissue engineering [21]. Self-assembled biotinylated pullulan acetate nanoparticles loading adriamycin were described as targeted anti-cancer drug delivery systems, internalized by HepG2 cells. The drug loading and release rate were accessed with a dialysis method [18]. Adriamycin loaded pullulan acetate/sulfonamide conjugate nanoparticles responding to tumor pH revealed pH-dependent cell interaction, internalization and cytotoxicity in *in vitro* studies using a breast tumor cell line (MCF-7). The drug loading profile was evaluated using a dialysis method [19]. Non-toxicity, efficient internalization and transfection *in vitro* of hydrogel pullulan nanoparticles encapsulating pBUDLacZ plasmid showed this system to be an efficient gene delivery carrier [14]. Pullulan potentially targets and accumulates in the liver because it is recognized by the asialoglycoprotein receptor expressed on the sinusoidal surface of the hepatocytes [22]. The asialoglycoprotein receptor was reported to be involved in pullulan receptor-mediated endocytosis [23].

The production of hydrophobically modified pullulan nanogels, using an approach similar to the one presented in this work, was achieved by other authors using cholesteryl group-bearing pullulan. The resulting nanogels were monodisperse, with a diameter of 20–30 nm and stable in water. Their size and density were controlled by the pullulan degree of substitution with cholesterol and the molecular weights of parent pullulan [24]. This nanogel was utilized in molecular complexation with bovine serum albumin (BSA) [25], insulin [26], lipase [27], human epidermal growth factor receptor 2 (HER-2) [28-30], interleukin-12 (IL-12) [31,32], among other therapeutic molecules, proving this system to be useful as a therapeutic delivery system. Self-assembled hydrogel nanoparticles of cholesterol-bearing pullulan spontaneously release insulin from the complex and thermal denaturation/aggregation were effectively suppressed upon complexation [26]. Cholesteryl group-bearing pullulan complexed with the truncated HER-2 protein, delivered a HER-2 oncoprotein containing an epitope peptide to the major histocompatibility complex class I pathway, and was able to induce CD8+ cytotoxic T lymphocytes against HER-2+ tumors and caused complete rejection of tumors. The results suggested this hydrophobized polysaccharide may help soluble proteins to induce cellular immunity with potential benefit in cancer prevention and cancer therapy [30]. The subcutaneous injection of cholesterol-bearing pullulan complexed with recombinant murine IL-12 led to a prolonged elevation of IL-12 concentration in the serum. Repetitive administrations of the

complex induced drastic growth retardation of reestablished subcutaneous fibrosarcoma, without causing toxicity [31]. Raspberry-like assembly of nanogels encapsulated IL-12 efficiently (96%) and kept it stable in the presence of BSA (50 mg/mL) and showed high potential to maintain a high IL-12 level in plasma after subcutaneous injection in mice [32]. Cationic derivative, ethylenediamine group functionalization of cholesteryl group-bearing pullulan, was developed as an effective intracellular protein delivery system [33]. The same research group designed hybrid hydrogels with self-assembled nanogels as cross-linkers to achieve interaction with proteins and chaperone-like activity [32,34,35]

Nanogel formulations, described as potential drug and vaccine delivery systems, have the potential to modify the drug, gene, protein, peptide, oligosaccharide or immunogen profile and the ability to cross biological barriers, the biodistribution and pharmacokinetics, improving their efficacy and safety, as well as the patient compliance [36].

2. Results and Discussion

In the present work, hydrophobized pullulan was obtained with a two-step synthesis. The resultant self-assembled nanogels were characterized in terms of structure, size, shape, surface charge and stability by hydrogen nuclear magnetic resonance (^{1}H NMR), fluorescence spectroscopy, cryo-field emission scanning electron microscopy (cryo-FESEM) and dynamic light scattering (DLS).

2.1. Synthesis of Pullulan-C_{16}

Scheme I. Synthesis of pullulan-C_{16}.

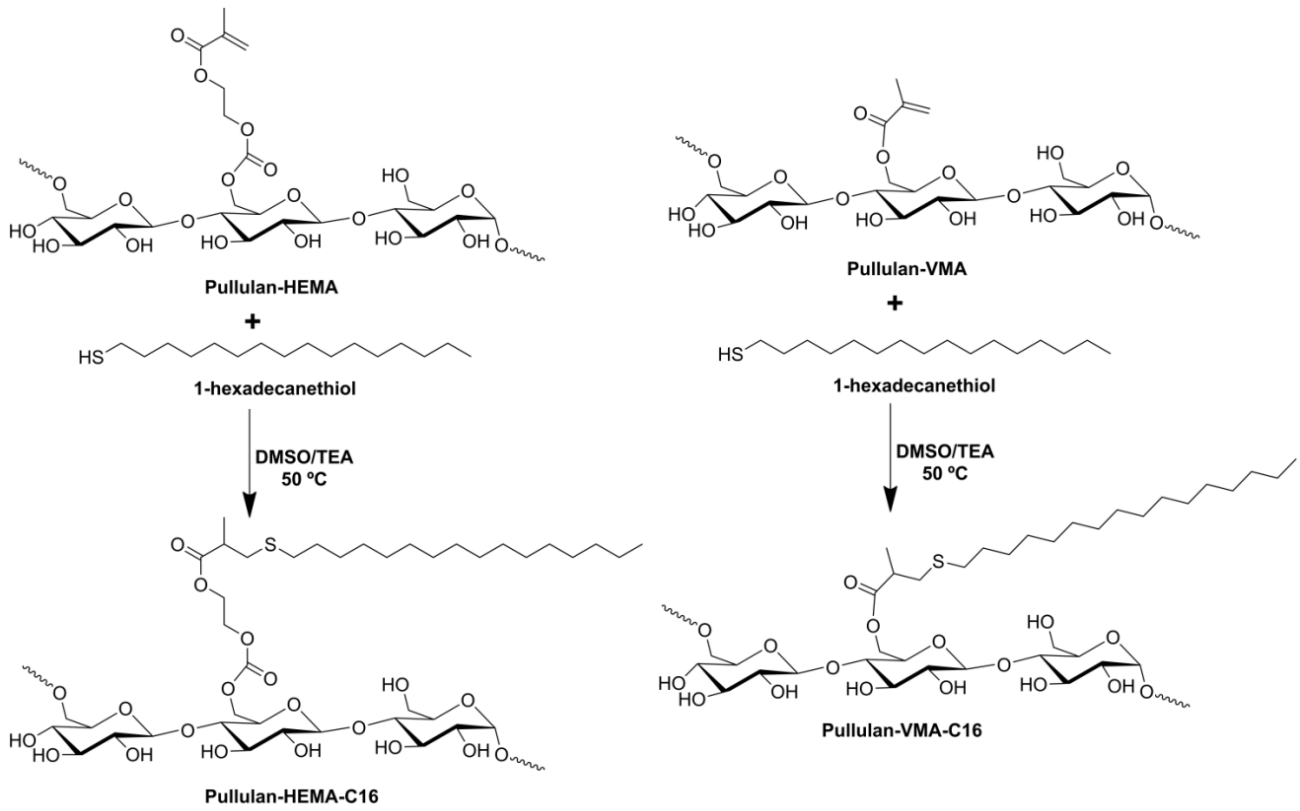

According to the literature and in the same way as other reported methacrylates, hydroxyethyl methacrylate (HEMA) and vinyl methacrylate (VMA) should be grafted on the ^{6}C of the glucose residues [37]. Then, by the Michael addition mechanism, the thiol from 1-hexadecanethiol (C_{16}) acting as a nucleophile reacts with grafted methacrylate (Scheme I). The success of the synthesis, purity, chemical structure and polymer degree of substitution of the reaction products were controlled using ^{1}H NMR spectra in deuterium oxide (D_2O) (Figure 1 and Table 1). Different independent batches of hydrophobized pullulan (pullulan-C_{16}) with various degree of substitution with the methacrylated groups and hydrophobic alkyl chains (DS_{HEMA} or DS_{VMA} and DS_{C16}, defined as the percentage of grafted HEMA or VMA or C_{16} moieties relative to the glucose residues, respectively), were synthesized by varying the molar ratios of methacrylate groups to glucose residues and the molar ratios of C_{16} to methacrylated groups. The synthetic procedure adopted proves to be versatile, simple and reproducible (Table 1).

Table 1. Characteristics of Pullulan-C_{16}.

***t*DS$_{HEMA}$ or *t*DS$_{VMA}$** [a]	**DS$_{HEMA}$ or DS$_{VMA}$** [b]	***t*DS$_{C16}$** [c]	**DS$_{C16}$** [d]	**DS$_{C16}$/DS$_{HEMA}$ or DS$_{C16}$/DS$_{VMA}$** [e]	**Pullulan-C$_{16}$** [f]
		Pullulan-HEMA-C_{16}			
20	5.6	120	1.3	23.2	PHC$_{16}$-5.6-1.3
25	8	80	4.6	57.5	PHC$_{16}$-8-4.6
		200	4.3	53.8	PHC$_{16}$-8-4.3
40	10	80	1.2	12	PHC$_{16}$-10-1.2
		200	5.9	59	PHC$_{16}$-10-5.9
		Pullulan-VMA-C_{16}			
25	8.8	200	6	68.2	PVC$_{16}$-8.8-6
50	10	200	7	70	PVC$_{16}$-10-7

[a] Theoretical DS_{HEMA} or DS_{VMA} calculated as the molar ratio of HEMA or VMA to glucose residue (×100) in the reaction mixture. [b] Calculated from the ^{1}H NMR spectra in D_2O of pullulan-HEMA or pullulan-VMA in D_2O with the equation $(I_a)/(I_{H1})\times100$, in which I_a is the average integral of the protons of the unsaturated carbons of the acrylate groups (around 6 ppm) [38,39] and I_{H1} is the integral of the anomeric protons (4.86, 5.28 and 5.30 ppm) [4,40]. [c] Theoretical DS_{C16} calculated as the molar ratio of C_{16} to methacrylated groups (×100) in the reaction mixture. [d] Calculated from the ^{1}H NMR spectra of pullulan-C_{16} in D_2O with the equation $(7X)/(37Y)\times100$, in which X is the average integral corresponding to the protons from alkyl moieties (1.8–0.6 ppm) [41] and Y is the integral of all pullulan protons (3.3–4.0 ppm and 4.86, 5.28 and 5.30 ppm) [4,40]. [e] Obtained DS_{C16} relative to methacrylated groups calculated using the following equation: DS_{C16}/DS_{HEMA} (×100) or DS_{C16}/DS_{VMA} (×100). [f] Pullulan-HEMA-SC_{16} synthesized: PHC$_{16}$-DS_{HEMA}-DS_{C16}; or Pullulan-VMA-SC_{16} synthesized: PVC$_{16}$-DS_{VMA}-DS_{C16}. The table presents the values (%) obtained in each set of conditions.

Figure 1. ^{1}H NMR spectra of (**a**) pullulan-HEMA and (**e**) pullulan-VMA in D_2O. ^{1}H NMR spectra of PHC_{16}-5.6-1.3 and PVC_{16}-10-7 in (**b**, **f**) DMSO-d_6, (**c**, **g**) 10% D_2O in DMSO-d_6 and (**d**, **h**) D_2O, respectively.

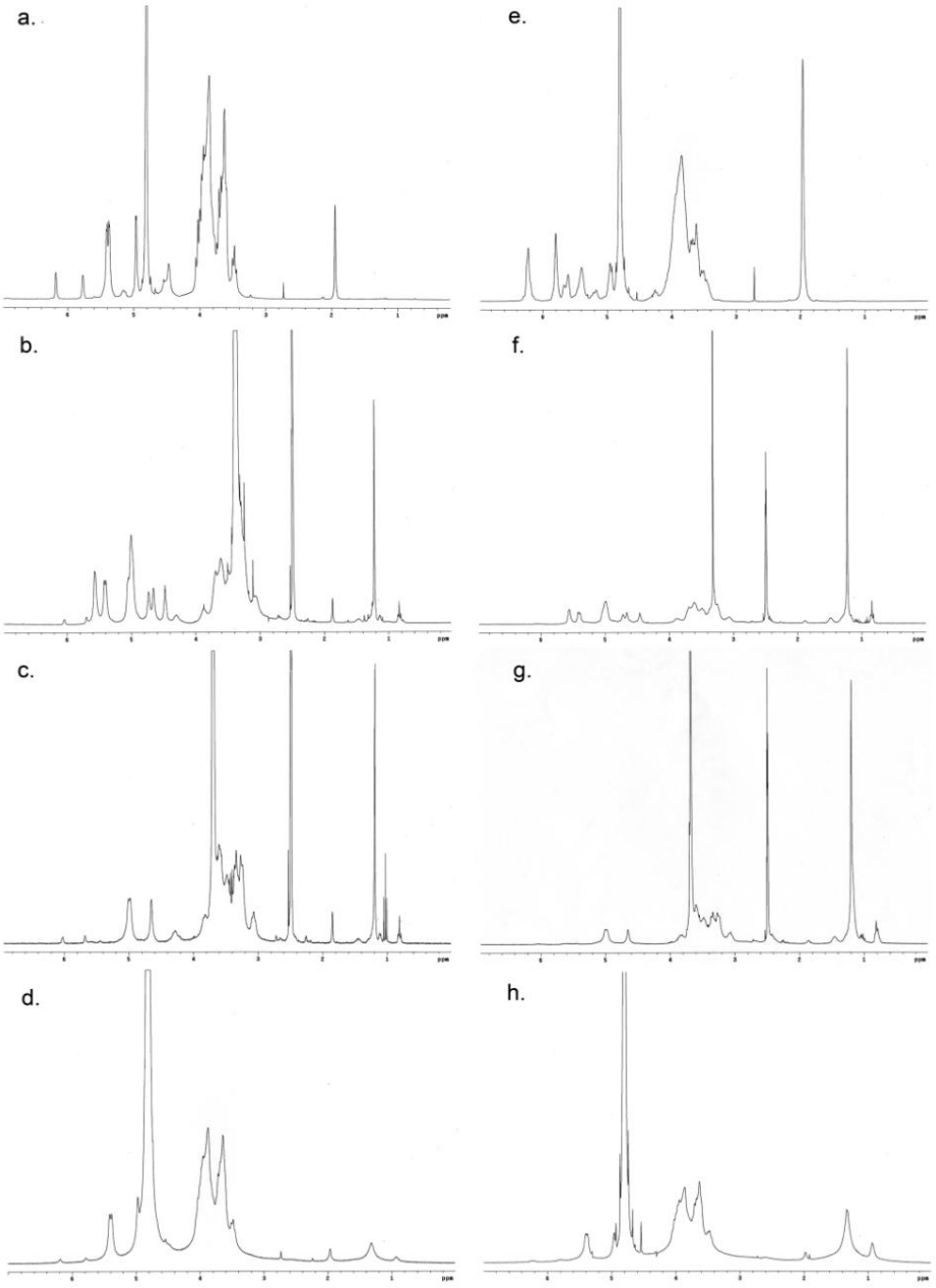

2.2. Self-assembly of Pullulan-C_{16}

The self-assembly of amphiphilic pullulan-C_{16} in water was studied using ^{1}H NMR and fluorescence spectroscopy. Analyzing the ^{1}H NMR spectra of pullulan-C_{16} (Figure 1), it can be observed that while the mobility of the polysaccharide skeleton was maintained in environments of different polarity, the shape and width of the proton signals of the methyl (0.8 ppm) and methylene (1.1 ppm) groups of C_{16} depended on the polarity of the solvent used. In dimethyl sulfoxide-d_6 (DMSO-d_6), pullulan-C_{16} was soluble, and the C_{16} signals were sharp, as all hydrophobic chains were

exposed to the solvent, having the same mobility (Figure 1b and 1f) [41]. Increasing the percentage of D_2O in DMSO-d_6, the base of those signals broadened (Figure 1c and 1g). In pure D_2O, a large broadening was obvious, which represents the superposition of peaks of chemically identical species, yet possessing various degrees of mobility (Figure 1d and 1h) [42]. These results give evidence that pullulan-C_{16} dispersed in water has part of the alkyl chains exposed to hydrophobic domains, while others might have been exposed to the hydrophilic solvent. Differences in the environment and/or mobility of the molecules thus explain the broad peak observed for the aliphatic protons. Therefore, pullulan-C_{16} nanogels are obtained upon self-assembly in water through the association of the hydrophobic alkyl chains in hydrophobic domains.

The critical aggregation concentration (cac) or critical micelle concentration (cmc) of pullulan-C_{16} was studied by fluorescence spectroscopy using hydrophobic dyes, Pyrene (Py) [43,44] and Nile red (NR) [45], whose solubility and fluorescence are weak in water but high in hydrophobic environments.

The intensity of Py increased with increasing concentrations of pullulan-C_{16}, and a red shift occurred in the excitation spectra (Figure 2a, 2b). Above cac, in the emission spectra (Figure 2a, 2b), some bands in the 450 nm region associated to the presence of Py dimers are detected in pullulan-C_{16}, suggesting high water penetration into the nanogel, which is in agreement with the ^{1}H NMR measurements. The intensity ratio of the third and first vibrational bands, I_3/I_1, rapidly augmented above the cac, which was 0.06 mg/mL for PHC$_{16}$-5.6-1.3 and for PVC$_{16}$-10-7. This transition of intensity translated the transference of Py to a less polar and hydrophobic domain that was coincident to the onset of supramolecular formation of pullulan-C_{16} nanogels (Figure 2c). A lower I_3/I_1 ratio obtained for PHC$_{16}$-5.6-1.3 indicates the location of Py in a more hydrophilic environment, while a higher I_3/I_1 ratio for PVC$_{16}$-10-7 indicates the location of Py in a more hydrophobic environment (Figure 2c) [43]. This is confirmed by a better defined vibronic structure of Py emission in the case of PVC$_{16}$-10-7. Surprisingly, the resulting cac is the same for both nanogels despite their different DS_{C16} relative to methacrylated groups (70% for PVC$_{16}$-10-7 and 23% for PHC$_{16}$-5.6-1.3).

The area-normalized fluorescence emission intensity of NR was constant, without any shift in the maximum emission wavelength, for lower concentrations of pullulan-C_{16} because individual molecules exist as premicelles in aqueous environment (Figure 3; zone A). In contrast, for concentrations greater than the cac, fluorescence intensity increased and the maximum emission wavelength was blue-shifted due to the transfer of NR to the hydrophobic domains of the nanogels. The resultant cac was 0.04 mg/mL and 0.01 mg/mL for PHC$_{16}$-5.6-1.3 and PVC$_{16}$-10-7, respectively (Figure 3). This variation is consistent with the C_{16} loading of the studied pullulan nanogels as higher hydrophobicity results in lower cac. The PVC$_{16}$-10-7 hydrophobic domains are dissimilar to those present in a typical surfactant system and have two types of hydration levels (Figure 3b; zones B and C), while in PHC$_{16}$-5.6-1.3 only a type of hydrophobic domains is observed (Figure 3a; zone C). This observation shows a slight dependence of the formed hydrophobic domains on the type of linker used (HEMA or VMA).

Figure 2. Determination of the critical aggregation concentration (cac) of pullulan-C_{16} using fluorescence excitation (λ_{em} = 390 nm) and emission (λ_{ex} = 339 nm) spectra of Py (6×10^{-7} M) in the pullulan-C_{16}/water system as a function of the (**a**) PHC_{16}-5.6-1.3 and (**b**) PVC_{16}-10-7 concentration; (**c**) Intensity ratio I_3/I_1 as a function of the pullulan-C_{16} concentration. The cac obtained for both materials was 0.06 mg/mL.

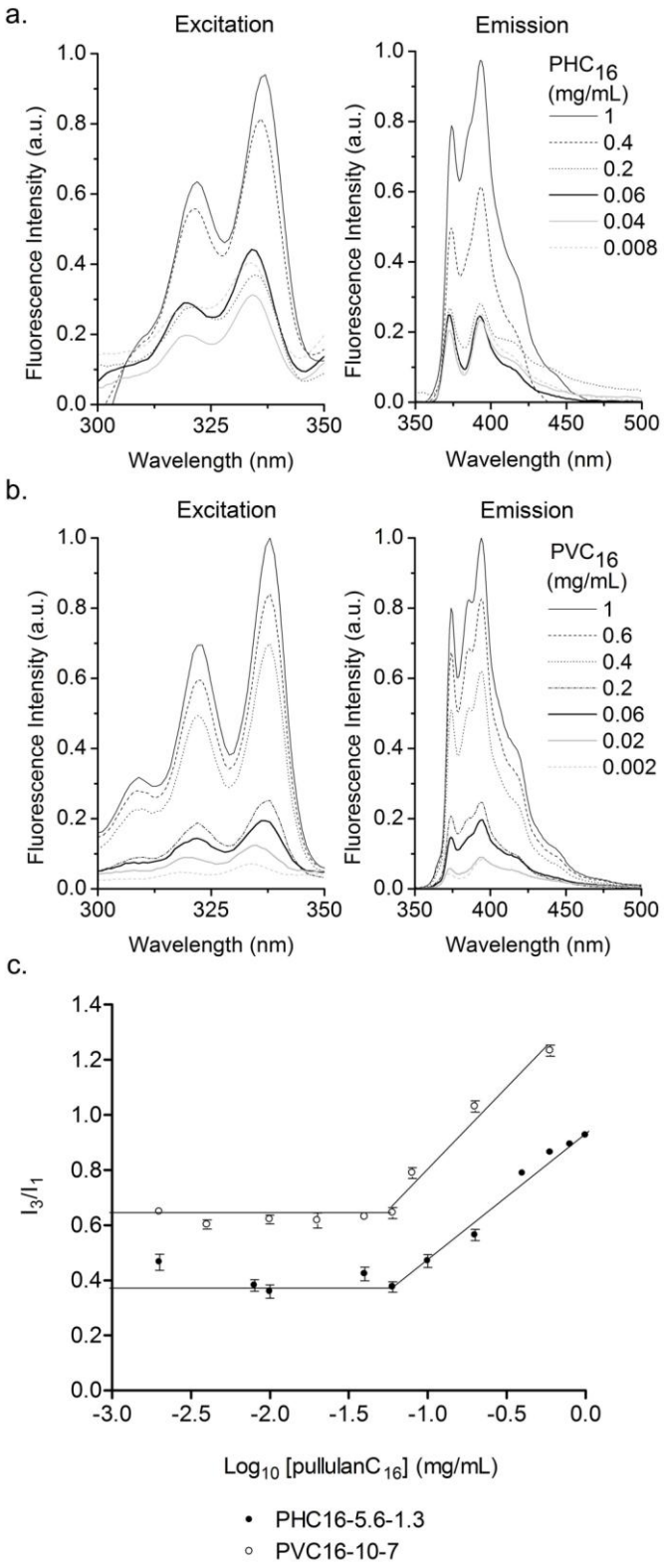

Figure 3. Determination of the cac of pullulan-C_{16} using area normalized fluorescence emission (λ_{ex} = 570 nm) spectra of NR (2×10^{-7} M) in the pullulan-C_{16}/water system as a function of (**a**) PHC_{16}-5.6-1.3 and (**b**) PVC_{16}-10-7 concentration; (**c**) area normalized fluorescence emission intensity and position of maximum emission wavelength of Nile red (NR) in the pullulan-C_{16}/water system as a function of pullulan-C_{16} concentration. The cac obtained for PHC_{16}-5.6-1.3 was 0.04 mg/mL and for PVC_{16}-10-7 was 0.01 mg/mL.

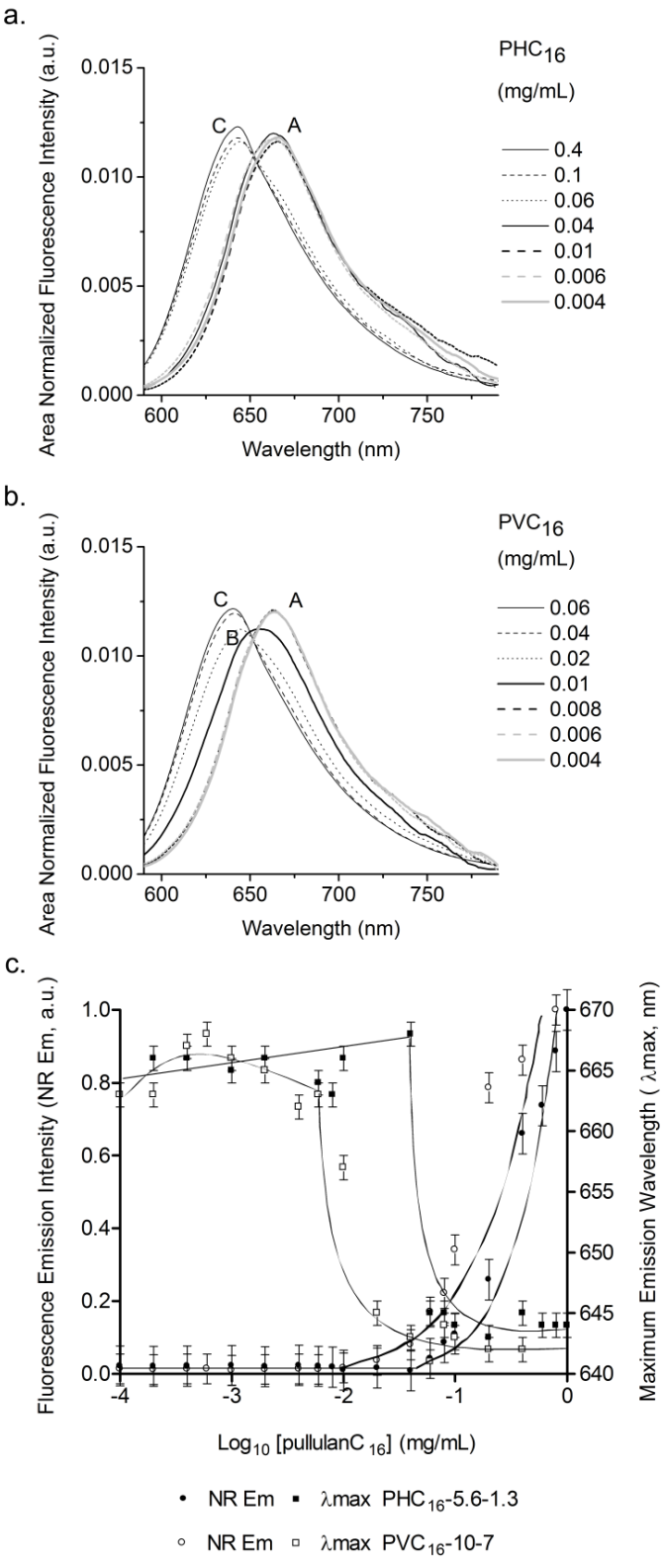

In the case of PHC_{16}-5.6-1.3, the determined cac values are similar for both fluorescent probes. But that is not the case for PVC_{16}-10-7. This is explainable by the fact that as Py molecules already start at a low hydrated pre-micellar environment they are unable to detect the micellar domains of type B, which have higher hydration levels than those domains of type C. For the last ones there is a sufficient variation of hydration level that can be detected by Py I_3/I_1 ratio resulting in a cac value above the real one. We thus conclude that NR is a more sensitive fluorescence probe as it was able to follow all the variations in hydration level that occurred in the self-aggregation process of PVC_{16}-10-7. For PHC_{16}-5.6-1.3 the absence of B type micellar domains and the higher hydration of the premicellar environment, also seen in NR emission in zone A, allowed compatible determinations of cac for both probes.

As pullulan-C_{16} concentration augments above the cac, more hydrophobic domains are formed, solubilizing more Py and NR, which consequently increases the fluorescence detected, not occurring the typical second plateau (Figures 2c, 3c). The highest concentration of pullulan-C_{16} used was insufficient to enclose all of the hydrophobic dyes—this might be caused by the continued redistribution of Py and NR molecules to the less hydrated hydrophobic domains and by the formation of Py dimers in the hydrophobic domains with greater hydration level.

2.3. Characterization of Pullulan-C_{16} Nanogels

2.3.1. Size and shape

The hydrophobic forces that sequester the hydrophobic chains in the core and the excluded volume repulsion between the chains mostly establish the micellar size [46]. The pullulan-C_{16} nanogels appeared spherical in cryo-FESEM micrographs, with a large size distribution in the range of 100–700 nm for PHC_{16}-5.6-1.3 and 200–300 nm for PVC_{16}-10-7 (Figure 4).

Figure 4. Cryo-FESEM negatively stained micrographs (magnification 30000×) of (**a**) PHC_{16}-5.6-1.3 and (**b**) PVC_{16}-10-7.

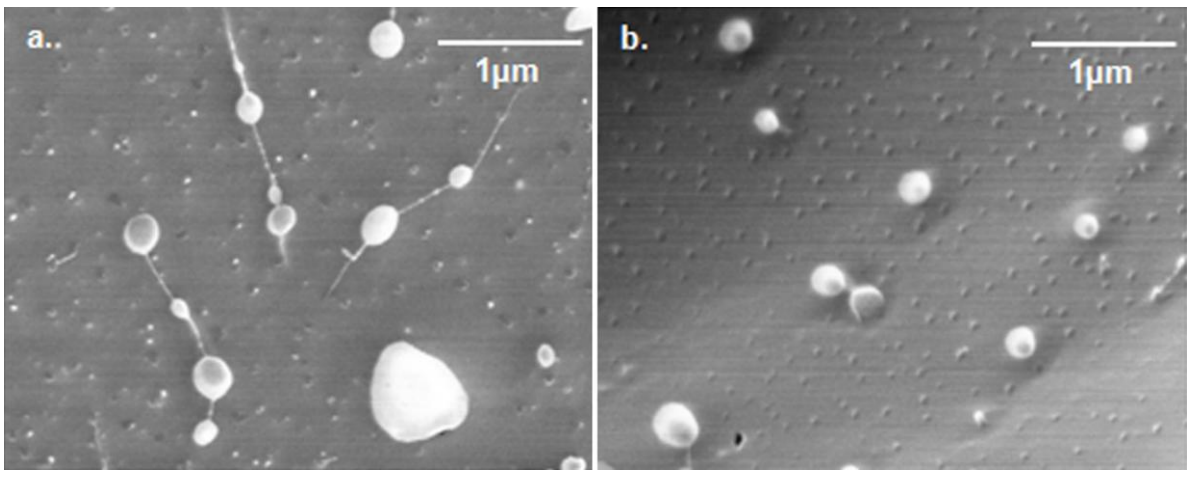

2.3.2. Storage

The mean hydrodynamic diameter obtained using DLS for pullulan-C_{16} nanogels dispersed in ultrapure water oscillated between 162 nm and 335 nm for PHC_{16}-5.6-1.3 and between 115 nm and 369 nm for PVC_{16}-10-7, over a six month storage period at room temperature (25 ℃). Both materials exhibited fairly high polydispersity, with an average pdI of 0.59 ± 0.11 for PHC_{16}-5.6-1.3 and 0.43 ± 0.23 for PVC_{16}-10-7, which means that there may be macromolecular micelles with a distribution of sizes and shapes, as also revealed by the cryo-FESEM micrographs (Figure 5).

Figure 5. Size of pullulan-C_{16} water dispersions (1 mg/mL) over a 6 month storage period at room temperature (25 ℃). Size was measured periodically in dynamic light scattering (DLS) (mean ± S.D., n = 10).

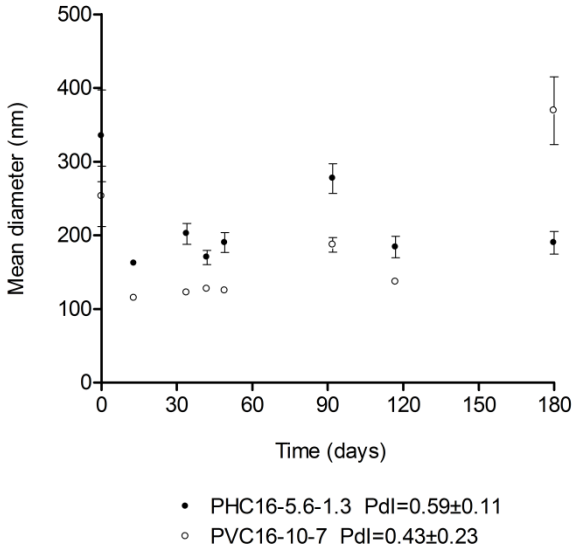

2.3.3. Effect of the Concentration of Pullulan-C_{16}

The mean hydrodynamic diameter tended to be much larger for lower concentrations of pullulan-C_{16}, especially when closer to the cac. It appears that, for higher concentrations of the polymer, the remaining solvent is gradually released from the hydrophobic core, resulting in a decrease in size. In contrast, occasionally exposed hydrophobic domains within a less mobile shell formed by hydrophilic chains may originate secondary aggregation enlarging the resultant macromolecular micelles [46]. The zeta-potential values were always negative and close to zero, never lower than −20 mV. Once zeta potential approaches zero, electrostatic repulsion becomes small compared to the ever-present Van der Waals attraction. In these conditions, eventually, instability may arise, causing aggregation followed by sedimentation and phase separation. However, the pullulan-C_{16} nanogels preserved their nanosize with the exception of PVC_{16}-10-7 at 0.5 mg/mL that formed aggregates out of the nanoscale (Figure 6).

Figure 6. Influence of concentration on the size and zeta potential of pullulan-C_{16} nanogels (0.05–2 mg/mL) measured at 37 °C in DLS (mean ± S.D., n = 3).

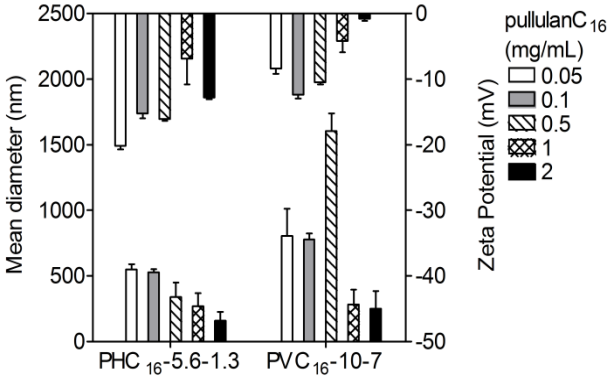

2.3.4. Effect of Urea

Urea is known for its ability to break intramolecular hydrogen bonds and to destabilize hydrophobic domains [47,48]. Urea and its derivatives are very efficient as modifiers of the aqueous solution properties participating at the level of the micellar solvation layer because it enhances the polarity and the hydrophilic character of water. An increased accessibility from the aqueous phase at higher urea concentrations could result in a stronger solvation of the polar groups in micellar aggregates by urea−water mixture than water alone. Urea is related to the enhancement of the solubility of hydrocarbon tails favoring their solvation and to the weakening of the hydrophobic interactions responsible for the formation and maintenance of the micellar assembly in aqueous solution. The action of urea on micellization depends on the way in which solvation occurs in a specific micellar system [49]. The results obtained show that urea did not affect the nanogel size of PHC_{16}-5.6-1.3. In contrast, urea caused concentration dependent destabilization of PVC_{16}-10-7, affecting the self-assembly of this amphiphilic system in water, leading to the formation of larger aggregates out of the nanoscale (Figure 7). Destabilization of PVC_{16}-10-7, resulting in higher particle size, may be tentatively assigned to improved solvation of the hydrophobic domains. This possibility is supported by the fact that PVC_{16} has a higher substitution degree than PHC_{16} (DS_{C16} of 7 *vs.* 1.3).

Figure 7. Influence of urea (0–7 M) on the size of pullulan-C_{16} nanogels (1 mg/mL) measured at 37 °C in DLS (mean ± S.D., n = 3).

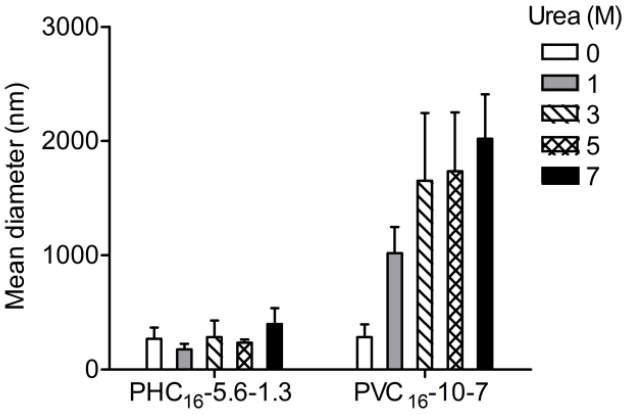

2.3.5. Effect of Ionic Strength

Colloidal stability might be compromised in the absence of an electrostatic barrier. The addition of enough quantity of salt neutralizes the surface charge of the micelles in dispersion and compresses the surface double layer, facilitating the colloidal aggregation. Without the repulsive forces that keep macromolecular micelles separate, coagulation might occur due to attractive Van der Waals forces. Compared to salt-free pullulan-C_{16} colloidal dispersion, while PHC_{16}-5.6-1.3 denoted stability, PVC_{16}-10-7 nanogel was larger as the ionic strength increased with increasing concentrations of NaCl (Figure 8).

Figure 8. Influence of NaCl (0–0.6 M) on the size of pullulan-C_{16} nanogels (1 mg/mL) measured at 37 ℃ in DLS (mean ± S.D., n = 3).

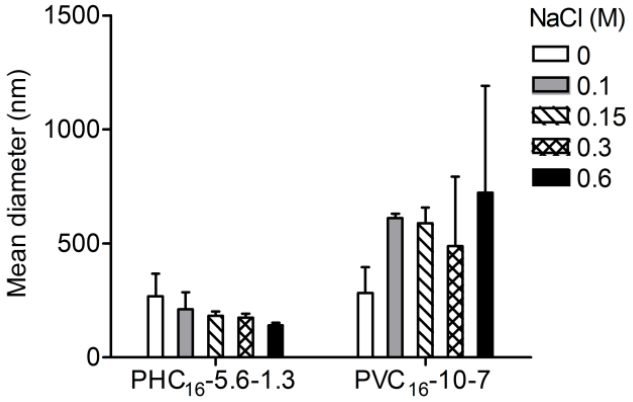

2.3.6. Effect of pH

Size distributions and zeta potential of pullulan-C_{16} as a function of pH, using phosphate-citrate buffer (pH 2.2–8.0), were compared to values obtained in water and PBS. The mean hydrodynamic diameter values obtained either for PHC_{16}-5.6-1.3 or PVC_{16}-10-7 were similar in the range of pH studied. The size stability, in the range of pH studied, demonstrates that the organization of hydrophobic alkyl chains, in hydrophobic domains with low water content, protect the amphiphilic molecules from the hydrolysis of the carbonate ester at alkaline pH and from the hydrolysis of the methacrylate ester at low pH [50]. For both materials, small negative values of zeta potential were obtained indicating little repulsion between macromolecular micelles to prevent aggregation. However, even with zeta potential close to zero, particles denoted only slight instability in the nanoscale (Figure 9). The nearly neutral charge is valuable for *in vivo* use, since large positively charged materials cause non-specific cell sticking, while large negatively charged materials are efficiently taken up by scavenger endothelial cells or “professional pinocytes” found in the liver, which results in a rapid clearance from the blood [51].

Figure 9. Influence of pH on the size and zeta potential of pullulan-C_{16} nanogels measured at 37 ℃ in DLS (mean ± S.D., n = 3).

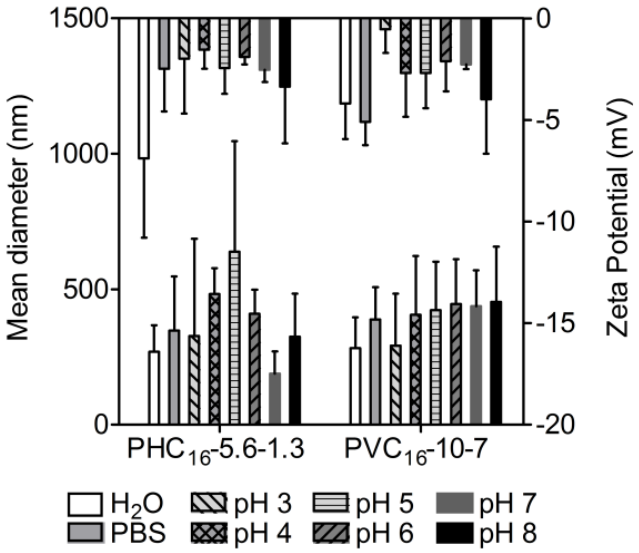

Pullulan-based nanogels synthesized and characterized in this work have high water content, tunable size, interior network for possible incorporation of therapeutics, and large surface area for potential multivalent bioconjugation with cell-targeting ligands such as protein, peptides and antibodies. With these characteristics, described nanogels might be useful as polymeric carriers for therapeutic targeted delivery.

In our laboratory several nanogels are being developed, using different polysaccharides: dextrin, mannan, hyaluronic acid, glycolchitosan. The use of different polysaccharides allows the production of nanogels bearing different surface properties, namely size, charge and bioactivity. Among the applications envisaged for these materials, 1) the delivery of therapeutic proteins and of poorly water soluble pharmaceuticals, 2) vaccination, and 3) delivery of nucleic acid therapeutics are being developed. The comprehensive characterization of several nanogels provides a platform for the development of more sophisticated materials, with ability to perform as delivery systems. Recent results in our laboratory demonstrate the potential of dextrin nanogels for the delivery of cytokines, namely IL-10 [52]; the association of the nanogels with injectable hydrogels is also a promising field of application of the self-assembled nanogels, allowing the incorporation of hydrophobic molecules in the highly hydrated environment of hydrogels. Ongoing work addresses the study of biodistribution and drainage of nanogels to the lymphatic nodes. Preliminary results using radioactively labeled nanogels and immunohistochemical analysis of the lymphatic nodes confirm the ability of the nanogels to reach the nodes, internalized in phagocytic cells. The use of mannan opens interesting possibilities concerning the use of the nanogels for vaccination purposes, acting as a delivery system and as an adjuvant. Self-assembled nanogels are thus very promising materials that bring together the essential requisites of biocompatibility and performance.

3. Experimental Section

3.1. Materials

CDI-activated hydroxyethyl methacrylate (HEMA-CI) was produced as described elsewhere [38]. Pullulan (Mw = 100,000 g/mol), vinyl methacrylate (VMA), dimethyl sulfoxide (DMSO), 4-(N,N-dimethylamino)pyridine (DMAP), triethylamine (TEA), 1-hexadecanethiol (C_{16}), deuterium oxide (D_2O), dimethyl sulfoxide-d_6 (DMSO-d_6), pyrene (Py), 9-(diethylamino)-5H-benzo[α]phenoxazin-5-one (Nile red, NR) were purchased from Sigma-Aldrich. Pyrene was purified by appropriate recrystallization from absolute ethanol. Phosphotungstic acid was purchased from Riedel-de Haën. Regenerated cellulose tubular membranes, with a 12000−14000 nominal MWCO, were obtained from Membrane Filtration Products. Water was purified with a Milli-Q system (Millipore) with resistivity equal to 18.2 MΩ.cm. Other organic and inorganic chemicals were purchased from Sigma-Aldrich and used without further purification.

3.2. Synthesis of Amphiphilic Pullulan-C_{16}

Hydroxyethyl methacrylate-derivatized pullulan (pullulan-HEMA) was prepared as described by Van Dijk-Wolthuis *et al.* [38]. Briefly, pullulan was dissolved in dry DMSO in a nitrogen atmosphere with different calculated amounts of HEMA-CI, resulting in 0.20, 0.25 and 0.4 molar ratios of HEMA-CI to glucose residues. The reaction catalyzed by DMAP (2 mol equiv to HEMA-CI) was allowed to proceed and the mixture was stirred at room temperature for 4 days. The reaction was terminated with concentrated HCl (2% v/v), which neutralized DMAP and imidazole. The mixture was then dialyzed against frequently changed distilled water at 4 °C for 3 days. After being lyophilized, pullulan-HEMA resulted as a white fluffy product, which was stored at −20 °C.

Vinyl methacrylated pullulan (pullulan-VMA) was synthesized by transesterification of pullulan with VMA, overall as described by Ferreira *et al.* [39] but without enzymes [53]. Briefly, pullulan was dissolved in dry DMSO, with calculated amounts of VMA resulting in 0.25 and 0.5 molar ratios of VMA to glucose residues. After stirring at 50 °C for 2 days, the resulting mixture was dialyzed for 3 days against frequently changed distilled water, at room temperature (~25 °C). Each sample of modified pullulan after being lyophilized resulted as a white fluffy product that was stored at room temperature.

Finally, the amphiphilic molecules pullulan-HEMA-C_{16} (PHC_{16}) and pullulan-VMA-C_{16} (PVC_{16}) were produced as described elsewhere [41]. In brief, Pullulan-HEMA or Pullulan-VMA reacted in dry DMSO (equivalent HEMA or VMA = 0.03 M) with C_{16}. The reaction was catalyzed by TEA in a 2 molar ratio of TEA to HEMA or VMA. After stirring for 3.5 days at 50 °C, the resulting mixture was dialyzed, lyophilized and stored as described above.

3.3. Characterization of pullulan-C_{16} nanogels

3.3.1. ^{1}H NMR Spectroscopy

Lyophilized reaction products were dispersed in D_2O (5 mg/mL). The pullulan-C_{16} was also dispersed in DMSO-d_6 and in 10% D_2O in DMSO-d_6 (5 mg/mL). Samples were stirred overnight at

50 ℃ to obtain a clear dispersion, which was transferred to 5 mm NMR tubes. One-dimensional ^{1}H NMR measurements were performed in a Varian Unity Plus 300 spectrometer operating at 299.94 MHz. One-dimensional ^{1}H NMR spectra were recorded at 298 K with 256 scans, a spectral width of 5000 Hz, a relaxation delay of 1 s between scans, and an acquisition time of 2.8 s.

3.3.2. Fluorescence Spectroscopy

The cac of the pullulan-C_{16} was fluorometrically investigated using hydrophobic guest molecules, such as Py and NR. The fluorescence intensity change of these guest molecules was calculated as a function of the pullulan-C_{16} concentration. Briefly, lyophilized pullulan-C_{16} was dispersed in ultrapure water (1 mg/mL) with stirring for 3–5 days at 50 ℃. Consecutive dilutions of 1mL of each sample were prepared in ultrapure water. In the case of Py, a volume of 5 μL of a 1.2×10^{-4} M Py stock solution in ethanol was added, giving a constant concentration of 6×10^{-7} M in 0.5 % ethanol/water for all Py fluorescence measurements. In case of NR, a volume of 5μL of a 4×10^{-5} M NR stock solution in ethanol was then added, giving a constant concentration of 2×10^{-7} M in 0.5 % ethanol/water for all NR fluorescence measurements. The samples were stirred overnight. Fluorescence measurements were performed with a Spex Fluorolog 3 spectrofluorimeter, at room temperature. The slit width was set at 5 nm for excitation and 5 nm for emission. All spectra were corrected for the instrumental response of the system. The signal obtained for each sample was subtracted with the signal obtained with negative control, which corresponded to pullulan derivatives at exactly the same experimental conditions but without the guest NR or Py molecules. The cac was calculated using both the Py fluorescence intensity ratio of the third (384–385 nm) and first vibrational bands (372–374 nm) (I_3/I_1) of the emission spectra (λ_{ex} = 339 nm) and the maximum emission intensity of NR (λ_{ex} = 570 nm) in the pullulan-C_{16}/water system as a function of pullulan-C_{16} concentration; in both cases, the cac was estimated as the interception of two trend lines.

3.3.3. Cryo-FESEM

Each colloidal dispersion of pullulan-C_{16} was prepared with stirring of the lyophilized pullulan-C_{16} in ultrapure water for 3–5 days at 50 ℃ (1 mg/mL) followed by filtration (pore size 0.45 μm), with insignificant material lost, as confirmed with the phenol-sulfuric acid method, using glucose as standard [54]. The colloidal dispersions were concentrated by ultrafiltration (Amicon Ultra-4 Centrifugal Filter Units, cutoff molecular weight 1×10^5) and negatively stained with phosphotungstic acid (0.01% w/v). Samples were placed into brass rivets, plunged frozen into slush nitrogen at −200 ℃ and transferred to the cryo stage (Gatan, Alto 2500, U.K.) of an electronic microscope (SEM/EDS: FESEM JEOL JSM6301F/Oxford Inca Energy 350). Each sample was fractured on the cryo stage with a knife. Once in the microscope, sublimation of ice was carried out in the cryo chamber for 10 min at −95 ℃, allowing the exposure of the nanogel particles. The samples were sputter coated with gold and palladium at −140 ℃, using an accelerating voltage of 10 kV. The antipollutant of copper covers and protects the sample. The samples were observed at −140 ℃ at 15 kV. The solvent used in the preparation of the samples (water and phosphotungstic acid) was also observed as a negative control.

3.3.4. DLS

The size distribution and zeta potential measurements for each colloidal dispersion, prepared as described above for cryo-FESEM, were performed in a Malvern Zetasizer NANO ZS (Malvern Instruments Limited, U.K.) using a He-Ne laser wavelength of 633 nm, a detector angle of 173 ° and a refractive index of 1.33.

Size. For each sample (1 mL), the polydispersity index (pdI) and z-average diameter, which corresponds to the mean hydrodynamic diameter, were evaluated in 10 repeated measurements performed periodically during 6 months of storage in a polystyrene cell at 25 ℃. The size distribution of each sample dispersed in ultrapure water (0.05–2 mg/mL), phosphate-buffered saline (PBS 1x, pH 7.4), phosphate-citrate buffer (pH 2.2–8.0), NaCl (0–0.6 M) or in urea (0–7 M) was executed at 37 ℃ in three independent experiments, three repeated measurements being performed in each one.

Zeta Potential. Each sample dispersed in ultrapure water (0.05–2 mg/mL), phosphate buffered saline (PBS 1x, pH 7.4) or in phosphate-citrate buffer (pH 2.2–8.0) was analyzed at 37 ℃ in a folded capillary cell. The zeta potential values reported were calculated using the Smoluchowski equation with three independent experiments, three repeated measurements being performed in each one.

4. Conclusions

Hydrophobized pullulan nanogels were designed with a versatile, simple, reproducible and low-cost method. Above the cac, upon self-assembly in water, spherical polydisperse macromolecular micelles revealed long-term size stability in aqueous medium, with a nearly neutral negative surface charge and mean hydrodynamic diameter in the range 162–335 nm for PHC_{16}-5.6-1.3 and 115–369 nm for PVC_{16}-10-7. Size and zeta potential stability of pullulanC_{16} nanogels was maintained when exposed to potential destabilizing conditions of pH. While the size stability of the nanogel made of VMA with C_{16} grafted, PVC_{16}-10-7, was affected by the ionic strength and urea, nanogel made of pullulan with HEMA and fewer C_{16} grafted, PHC_{16}-5.6-1.3, remained more stable.

Pullulan-based nanogels have tunable size, high water content, interior network for possible incorporation of therapeutics, and large surface area for potential multivalent bioconjugation with cell-targeting ligands. With these characteristics, described nanogels might be useful as polymeric carriers for therapeutic targeted delivery. Further work is required to study molecular complexation, functionality and biocompatibility of these novel promising nanogels as drug and vaccine delivery systems.

Acknowledgements

We thank for the financial support by International Iberian Nanotechnology Laboratory (INL) and FCT through POCTI.

References

1. Catley, B.J.; Whelan, W.J. Observations on the structure of pullulan. *Arch. Biochem. Biophys.* **1971**, *143*, 138-142.

2. Colson, P.; Jennings, H.J.; Smith, I.C. Composition, sequence, and conformation of polymers and oligomers of glucose as revealed by carbon-13 nuclear magnetic resonance. *J. Am. Chem. Soc.* **1974**, *96*, 8081-8087.
3. Kasaai, M.R. Intrinsic viscosity-molecular weight relationship and hydrodynamic volume for pullulan. *J. Appl. Polym. Sci.* **2006**, *100*, 4325-4332.
4. Jiao, Y.H.; Fu, Y.; Jiang, Z.H. Synthesis and characterization of poly(ethylene glycol) grafted on pullulan. *Abstr. Paper Am. Chem. Soc.* **2003**, *225*, U576-U576.
5. Masuda, K.; Sakagami, M.; Horie, K.; Nogusa, H.; Hamana, H.; Hirano, K. Evaluation of carboxymethylpullulan as a novel carrier for targeting immune tissues. *Pharm. Res.* **2001**, *18*, 217-223.
6. Kimoto, T.; Shibuya, T.; Shiobara, S. Safety studies of a novel starch, pullulan: Chronic toxicity in rats and bacterial mutagenicity. *Food Chem. Toxicol.* **1997**, *35*, 323-329.
7. Shingel, K.I. Current knowledge on biosynthesis, biological activity, and chemical modification of the exopolysaccharide, pullulan. *Carbohydr. Res.* **2004**, *339*, 447-460.
8. Nomura, Y.; Ikeda, M.; Yamaguchi, N.; Aoyama, Y.; Akiyoshi, K. Protein refolding assisted by self-assembled nanogels as novel artificial molecular chaperone. *FEBS Lett.* **2003**, *553*, 271-276.
9. Shingel, K.I.; Petrov, P.T. Behavior of gamma-ray-irradiated pullulan in aqueous solutions of cationic (cetyltrimethylammonium hydroxide) and anionic (sodium dodecyl sulfate) surfactants. *Colloid Polym. Sci.* **2002**, *280*, 176-182.
10. Leathers, T.D. Biotechnological production and applications of pullulan. *Appl. Microbiol. Biotechnol.* **2003**, *62*, 468-473.
11. Hasuda, H.; Kwon, O.H.; Kang, I.K.; Ito, Y. Synthesis of photoreactive pullulan for surface modification. *Biomaterials* **2005**, *26*, 2401-2406.
12. Ito, Y.; Nogawa, M. Preparation of a protein micro-array using a photo-reactive polymer for a cell-adhesion assay. *Biomaterials* **2003**, *24*, 3021-3026.
13. Hosseinkhani, H.; Aoyama, T.; Ogawa, O.; Tabata, Y. Liver targeting of plasmid DNA by pullulan conjugation based on metal coordination. *J. Contr. Release* **2002**, *83*, 287-302.
14. Gupta, M.; Gupta, A.K. Hydrogel pullulan nanoparticles encapsulating pBUDLacZ plasmid as an efficient gene delivery carrier. *J. Contr. Release* **2004**, *99*, 157-166.
15. Akiyoshi, K.; Kobayashi, S.; Shichibe, S.; Mix, D.; Baudys, M.; Kim, S.W.; Sunamoto, J. Self-assembled hydrogel nanoparticle of cholesterol-bearing pullulan as a carrier of protein drugs: Complexation and stabilization of insulin. *J. Contr. Release* **1998**, *54*, 313-320.
16. Suginoshita, Y.; Tabata, Y.; Matsumura, T.; Toda, Y.; Nabeshima, M.; Moriyasu, F.; Kada, Y.; Chiba, T. Liver targeting of human interferon-beta with pullulan based on metal coordination. *J. Contr. Release* **2002**, *83*, 75-88.
17. Nogusa, H.; Yamamoto, K.; Yano, T.; Kajiki, M.; Hamana, H.; Okuno, S. Distribution characteristics of carboxymethylpullulan-peptide-doxorubicin conjugates in tumor-bearing rats: Different sequence of peptide spacers and doxorubicin contents. *Biol. Pharm. Bull.* **2000**, *23*, 621-626.
18. Na, K.; Bum Lee, T.; Park, K.H.; Shin, E.K.; Lee, Y.B.; Choi, H.K. Self-assembled nanoparticles of hydrophobically-modified polysaccharide bearing vitamin H as a targeted anti-cancer drug delivery system. *Eur. J. Pharm. Sci.* **2003**, *18*, 165-173.

19. Na, K.; Seong Lee, E.; Bae, Y.H. Adriamycin loaded pullulan acetate/sulfonamide conjugate nanoparticles responding to tumor pH: pH-dependent cell interaction, internalization and cytotoxicity in vitro. *J. Contr. Release* **2003**, *87*, 3-13.
20. Hasegawa, U.; Nomura, S.M.; Kaul, S.C.; Hirano, T.; Akiyoshi, K. Nanogel-quantum dot hybrid nanoparticles for live cell imaging. *Biochem. Biophys. Res. Commun.* **2005**, *331*, 917-921.
21. Na, K.; Shin, D.; Yun, K.; Park, K.H.; Lee, K.C. Conjugation of heparin into carboxylated pullulan derivatives as an extracellular matrix for endothelial cell culture. *Biotechnol. Lett.* **2003**, *25*, 381-385.
22. Yamaoka, T.; Tabata, Y.; Ikada, Y. Body distribution profile of polysaccharides after intravenous administration. *Drug Deliv.* **1993**, *1*, 75-82.
23. Kaneo, Y.; Tanaka, T.; Nakano, T.; Yamaguchi, Y. Evidence for receptor-mediated hepatic uptake of pullulan in rats. *J. Contr. Release* **2001**, *70*, 365-373.
24. Akiyoshi, K.; Deguchi, S.; Moriguchi, N.; Yamaguchi, S.; Sunamoto, J. Self-Aggregates of Hydrophobized Polysaccharides in Water—Formation and Characteristics of Nanoparticles. *Macromolecules* **1993**, *26*, 3062-3068.
25. Nishikawa, T.; Akiyoshi, K.; Sunamoto, J. Macromolecular complexation between bovine serum albumin and the self-assembled hydrogel nanoparticle of hydrophobized polysaccharides. *J. Am. Chem. Soc.* **1996**, *118*, 6110-6115.
26. Akiyoshi, K.; Kobayashi, S.; Shichibe, S.; Mix, D.; Baudys, M.; Kim, S.W.; Sunamoto, J. Self-assembled hydrogel nanoparticle of cholesterol-bearing pullulan as a carrier of protein drugs: Complexation and stabilization of insulin. *J. Contr. Release* **1998**, *54*, 313-320.
27. Sawada, S.I.; Akiyoshi, K. Nano-Encapsulation of Lipase by Self-Assembled Nanogels: Induction of High Enzyme Activity and Thermal Stabilization. *Macromol. Biosci.* **2010**, *10*, 353-358.
28. Kitano, S.; Kageyama, S.; Nagata, Y.; Miyahara, Y.; Hiasa, A.; Naota, H.; Okumura, S.; Imai, H.; Shiraishi, T.; Masuya, M.; Nishikawa, M.; Sunamoto, J.; Akiyoshi, K.; Kanematsu, T.; Scott, A. M.; Murphy, R.; Hoffman, E.W.; Old, L.J.; Shiku, H. HER2-specific T-cell immune responses in patients vaccinated with truncated HER2 protein complexed with nanogels of cholesteryl pullulan. *Clin. Cancer Res.* **2006**, *12*, 7397-7405.
29. Gu, X.G.; Schmitt, M.; Hiasa, A.; Nagata, Y.; Ikeda, H.; Sasaki, Y.; Akiyoshi, K.; Sunamoto, J.; Nakamura, H.; Kuribayashi, K.; Shiku, H. A novel hydrophobized polysaccharide/oncoprotein complex vaccine induces in vitro and *in vivo* cellular and humoral immune responses against HER2-expressing murine sarcomas. *Cancer Res.* **1998**, *58*, 3385-3390.
30. Shiku, H.; Wang, L.; Ikuta, Y.; Okugawa, T.; Schmitt, M.; Gu, X.; Akiyoshi, K.; Sunamoto, J.; Nakamura, H. Development of a cancer vaccine: Peptides, proteins, and DNA. *Cancer Chemother. Pharmacol.* **2000**, *46*, S77-82.
31. Shimizu, T.; Kishida, T.; Hasegawa, U.; Ueda, Y.; Imanishi, J.; Yamagishi, H.; Akiyoshi, K.; Otsuji, E.; Mazda, O. Nanogel DDS enables sustained release of IL-12 for tumor immunotherapy. *Biochem. Biophys. Res. Commun.* **2008**, *367*, 330-335.
32. Hasegawa, U.; Sawada, S.; Shimizu, T.; Kishida, T.; Otsuji, E.; Mazda, O.; Akiyoshi, K. Raspberry-like assembly of cross-linked nanogels for protein delivery. *J. Contr. Release* **2009**, *140*, 312-317.

33. Ayame, H.; Morimoto, N.; Akiyoshi, K. Self-assembled cationic nanogels for intracellular protein delivery. *Bioconjugate Chem.* **2008**, *19*, 882-890.
34. Morimoto, N.; Endo, T.; Iwasaki, Y.; Akiyoshi, K. Design of hybrid hydrogels with self-assembled nanogels as cross-linkers: interaction with proteins and chaperone-like activity. *Biomacromolecules* **2005**, *6*, 1829-1834.
35. Hirakura, T.; Yasugi, K.; Nemoto, T.; Sato, M.; Shimoboji, T.; Aso, Y.; Morimoto, N.; Akiyoshi, K. Hybrid hyaluronan hydrogel encapsulating nanogel as a protein nanocarrier: New system for sustained delivery of protein with a chaperone-like function. *J. Contr. Release* **2010**, *142*, 483-489.
36. Gonçalves, C.; Pereira, P.; Gama, M. Self-Assembled Hydrogel Nanoparticles for Drug Delivery Applications. *Materials* **2010**, *3*, 1420-1460.
37. Masci, G.; Bontempo, D.; Crescenzi, V. Synthesis and characterization of thermoresponsive N-isopropylacrylamide/methacrylated pullulan hydrogels. *Polymer* **2002**, *43*, 5587-5593.
38. vanDijkWolthuis, W.N.E.; Tsang, S.K.Y.; KettenesvandenBosch, J.J.; Hennink, W.E. A new class of polymerizable dextrans with hydrolyzable groups: Hydroxyethyl methacrylated dextran with and without oligolactate spacer. *Polymer* **1997**, *38*, 6235-6242.
39. Ferreira, L.; Gil, M.H.; Dordick, J.S. Enzymatic synthesis of dextran-containing hydrogels. *Biomaterials* **2002**, *23*, 3957-3967.
40. Glinel, K.; Sauvage, J.P.; Oulyadi, H.; Huguet, J. Determination of substituents distribution in carboxymethylpullulans by NMR spectroscopy. *Carbohydr. Res.* **2000**, *328*, 343-354.
41. Goncalves, C.; Martins, J.A.; Gama, F.M. Self-assembled nanoparticles of dextrin substituted with hexadecanethiol. *Biomacromolecules* **2007**, *8*, 392-398.
42. Hrkach, J.S.; Peracchia, M.T.; Domb, A.; Lotan, N.; Langer, R. Nanotechnology for biomaterials engineering: Structural characterization of amphiphilic polymeric nanoparticles by H-1 NMR spectroscopy. *Biomaterials* **1997**, *18*, 27-30.
43. Kalyanasundaram, K.; Thomas, J.K. Environmental Effects on Vibronic Band Intensities in Pyrene Monomer Fluorescence and Their Application in Studies of Micellar Systems. *J. Am. Chem. Soc.* **1977**, *99*, 2039-2044.
44. Dong, D.C.; Winnik, M.A. The Py Scale of Solvent Polarities. Solvent effects on the vibrionic fine structure of pyrene fluorescence and empirical correlations with ET and Y values. *Can. J. Chem.* **1984**, *62*, 2560-2565.
45. Coutinho, P.J.G.; Castanheira, E.M.S.; Rei, M.C.; Oliveira, M.E.C.D.R. Nile red and DCM fluorescence Anisotropy studies in C12E7/DPPC mixed systems. *J. Phys. Chem. B* **2002**, *106*, 12841-12846.
46. Jones, M.C.; Leroux, J.C. Polymeric micelles—A new generation of colloidal drug carriers. *Eur. J. Pharm. Biopharm.* **1999**, *48*, 101-111.
47. Mukerjee, P.; Ray, A. Effect of Urea on Micelle Formation and Hydrophobic Bonding. *J. Phys. Chem.* **1963**, *67*, 190-192.
48. Moore, D.R.; Mathias, L.J. Molecular Composites Via Insitu Polymerization - Poly(Phenylene Terephthalamide)-Nylon 3. *J. Appl. Polym. Sci.* **1986**, *32*, 6299-6315.

49. Hierrezuelo, J.M.; Molina-Bolívar, J.A.; Carnero Ruiz, C. On the Urea Action Mechanism: A Comparative Study on the Self-Assembly of Two Sugar-Based Surfactants. *J. Phys. Chem. B* **2009**, *113*, 7178-7187.
50. Dijk-Wolthuis, W.N.E.v.; Steenbergen, M.J.v.; Underberg, W.J.M.; Hennink, W.E. Degradation kinetics of methacrylated dextrans in aqueous solution. *J. Pharm. Sci.* **1997**, *86*, 413-417.
51. Smedsrod, B. Clearance function of scavenger endothelial cells. *Comp. Hepatol.* **2004**, *3*, S22.
52. Carvalho, V.; Castanheira, P.; Faria, T.Q.; Goncalves, C.; Madureira, P.; Faro, C.; Domingues, L.; Brito, R.M.; Vilanova, M.; Gama, M. Biological activity of heterologous murine interleukin-10 and preliminary studies on the use of a dextrin nanogel as a delivery system. *Int. J. Pharm.* **2010**, *400*, 234-242.
53. Carvalho, J.; Goncalves, C.; Gil, A.M.; Gama, F.M. Production and characterization of a new dextrin based hydrogel. *Eur. Polym. J.* **2007**, *43*, 3050-3059.
54. Dubois, M.; Gilles, K.A.; Hamilton, J.K.; Rebers, P.A.; Smith, F. Colorimetric Method for Determination of Sugars and Related Substances. *Anal. Chem.* **1956**, *28*, 350-356.